Biochemical and Biophysical Research Communications 450 (2014) 588–592

Contents lists available at ScienceDirect

Biochemical and Biophysical Research Communications

journal homepage: www.elsevier.com/locate/ybbrc

Adipogenesis stimulates the nuclear localization of EWS with an increase in its *O*-GlcNAc glycosylation in 3T3-L1 cells

Qiang Li, Kazuo Kamemura *

Department of Bioscience, Nagahama Institute of Bio-Science and Technology, 1266 Tamura, Nagahama, Shiga 526-0829, Japan

ARTICLE INFO

Article history:
Received 22 May 2014
Available online 10 June 2014

Keywords:
Ewing sarcoma proto-oncoprotein
Nuclear localization
3T3-L1
Adipogenesis
O-GlcNAc
Glycosylation

ABSTRACT

Although the Ewing sarcoma (EWS) proto-oncoprotein is found in the nucleus and cytosol and is associated with the cell membrane, the regulatory mechanisms of its subcellular localization are still unclear. Here we found that adipogenic stimuli induce the nuclear localization of EWS in 3T3-L1 cells. Tyrosine phosphorylation in the C-terminal PY-nuclear localization signal of EWS was negative throughout adipogenesis. Instead, an adipogenesis-dependent increase in *O*-linked β-*N*-acetylglucosamine (*O*-GlcNAc) glycosylation of EWS was observed. Pharmacological inactivation of *O*-GlcNAcase in preadipocytes promoted perinuclear localization of EWS. Our findings suggest that the nuclear localization of EWS is partly regulated by the glycosylation.

1. Introduction

The Ewing sarcoma (EWS) proto-oncoprotein is one of the three members of the FET (FUS/EWS/TAF15) family of RNA-binding proteins. Although EWS has been suggested to play multiple roles in transcription [1–3] and RNA processing and transport [4–9], the precise control of its multiple functions remains to be elucidated. EWS is found in both the nucleus and cytosol [2,10–14] and associates with the cell membrane [15]. Therefore, the physiological functions of EWS may be accomplished in part by its spatio-temporal dynamic subcellular distribution; however, the regulatory mechanisms of the subcellular localization of EWS are less clear.

Here, we show the adipogenesis-dependent dynamic subcellular distribution of EWS in 3T3-L1 cells. The nuclear distribution of EWS took precedence over its cytosolic localization during adipogenic differentiation, while the majority of EWS was distributed to the cytosol in preadipocytes. Our results also indicate that the adipogenesis-dependent increase in *O*-linked β-*N*-acetylglucosamine (*O*-GlcNAc) glycosylation of EWS has a regulatory role in its nuclear localization.

2. Materials and methods

2.1. Materials

Anti-EWS (SAB2500370) and anti-α-tubulin (B-5-1-2) antibodies were obtained from Sigma–Aldrich (St. Louis, MO). Antibodies against the following antigens were obtained from Santa Cruz Biotechnology (Santa Cruz, CA): EWS (G-5), β-actin (I-19), lamin B (M-20), and FLAG (M2). The anti-*O*-GlcNAc (CTD110.6) antibody was a kind gift from Dr. Gerald W. Hart (Johns Hopkins University School of Medicine, Baltimore, MD). The anti-phospho-tyrosine antibody (P-Tyr-100) was obtained from Cell Signaling Technology (Beverley, MA). Horseradish peroxidase (HRP)-conjugated anti-mouse IgG and HRP-anti-rabbit IgG antibodies were obtained from GE Healthcare (Buckinghamshire, UK), and the HRP-anti-goat IgG antibody was obtained from R & D Systems (Minneapolis, MN). Leptomycin B was obtained from Alomone Labs (Jerusalem, Israel). Sodium orthovanadate was obtained from Santa Cruz Biotechnology. Thiamet G was obtained from Cayman Chemical (Ann Arbor, MI).

2.2. Cell culture

Mouse 3T3-L1 preadipocytes were grown in Dulbecco's modified Eagle's medium (DMEM) containing 25 mM glucose supplemented with 10% (v/v) heat-inactivated bovine serum and were differentiated as reported previously [16]. Human embryonic kidney 293T cells were maintained in DMEM containing 5.5 mM

Abbreviations: DMEM, Dulbecco's modified Eagle's medium; EWS, Ewing sarcoma proto-oncoprotein; HRP, horseradish peroxidase; NLS, nuclear localization signal; *O*-GlcNAc, *O*-linked β-*N*-acetylglucosamine; PBS, phosphate-buffered saline.

* Corresponding author. Fax: +81 749 64 8140.
E-mail address: k_kamemura@nagahama-i-bio.ac.jp (K. Kamemura).

http://dx.doi.org/10.1016/j.bbrc.2014.06.013
0006-291X/

glucose supplemented with 10% (v/v) heat-inactivated fetal bovine serum at 37 °C in humidified air with 5% CO_2.

2.3. Oil red O staining

The cells were fixed with 10% formalin in phosphate-buffered saline (PBS) for 15 min. After 2 washes in PBS, the cells were stained for 1 h by adding a freshly diluted oil red O solution (6 parts 3% [w/v] oil red O in 2-propanol and 4 parts H_2O). After staining, the cells were washed with PBS and counterstained with Harris hematoxylin solution.

2.4. Subcellular fractionation

Approximately 1.0×10^6 cells were resuspended on ice in 800 μL of 10 mM HEPES (pH 7.9), 10 mM KCl, 0.1 mM EDTA, 0.1 mM EGTA, 1 mM DTT, and protease inhibitor cocktail (Nacalai Tesque, Kyoto, Japan) and incubated for 15 min. The suspension was added to 50 μL of 10% (w/v) Nonidet P-40 and vortexed vigorously for 10 s. The homogenate was centrifuged for 30 s at 1000×*g* and the supernatant was referred to as the cytosolic fraction. The pellet was resuspended in 100 μL of 20 mM HEPES (pH 7.9), 0.4 M NaCl, 1 mM EDTA, 1 mM EGTA, 1 mM DTT, and protease inhibitor cocktail and rocked vigorously at 4 °C for 15 min. The extract was centrifuged for 5 min at 10,000×*g* and the supernatant was referred to as the nuclear fraction.

2.5. Immunoprecipitation

For immunoprecipitation of EWS, cell lysates or subcellular fractions were incubated with the anti-EWS (G-5) antibody for 2 h at 4 °C. The immune complexes were precipitated with protein A/G PLUS-agarose (Santa Cruz Biotechnology) and washed extensively with 50 mM Tris–HCl (pH 7.5) and 154 mM NaCl. For the elution of proteins, the immune complexes were suspended in SDS–polyacrylamide gel electrophoresis sample buffer and boiled for 5 min.

2.6. Western blotting and statistical analysis

For the detection of proteins in western blots, the proteins were separated in an SDS–polyacrylamide gel, electroblotted onto a polyvinylidene difluoride membrane (Millipore, Bedford, MA), and subjected to immunodetection using the appropriate primary antibody. Proteins were visualized using an HRP-conjugated secondary antibody and enhanced chemiluminescence. Relative EWS levels were calculated by densitometry of the immunoblots. Statistical analysis was performed by Student's *t* test. A p value <0.05 (two-tailed) was considered significant. Data are presented as the mean ± standard deviation.

2.7. Immunocytochemistry

The cells were fixed with 4% formaldehyde in PBS for 15 min and permeabilized with 0.5% Triton X-100 in PBS for 15 min. After 2 washes with PBS, the cells were incubated for 1 h with PBS containing 4% FBS for blocking, and incubated overnight at 4 °C with the anti-EWS (SAB2500370) antibody diluted in PBS containing 4% FBS. The cells were washed once with PBS and incubated with an Alexa Fluor 488-conjugated anti-goat IgG antibody (Life Technologies, Carlsbad, CA) diluted in PBS for 2 h. The nuclei were stained with DAPI, and the samples were analyzed using an epifluorescence microscope.

3. Results and discussion

3.1. The majority of EWS proto-oncoprotein is regulated to localize stably in the cytosol in 3T3-L1 preadipocytes

EWS is an almost ubiquitously expressed protein among tissues and localizes mainly in the nucleus in the majority of tissues and cell types [12]. On the contrary, we found that the majority of EWS was distributed in the cytosol and a trace amount was detected in the nucleus using biochemical subcellular fractionation of 3T3-L1 preadipocytes (Fig. 1). Despite the fact that the nuclear localization signal (NLS) of EWS has been well-characterized [2,11,14], its nuclear export signal is unknown. We then examined the effect of leptomycin B, a CRM1/exportin 1 inhibitor, on the subcellular localization of EWS in 3T3-L1 preadipocytes (Fig. 1). Following 10 min of leptomycin B treatment, we observed an approximately 20% increase in the amount of nuclear EWS, and the nuclear ratio was kept constant until 120 min after treatment (Fig. 1). This result indicates that a proportion of EWS shuttles between the cytosol and nucleus and is exported from the nucleus to the cytosol in a CRM1/exportin 1-dependent manner, but the majority of EWS is resident in the cytosol in 3T3-L1 preadipocytes. Therefore, it is considered that the majority of EWS is regulated to localize stably in the cytosol in 3T3-L1 preadipocytes.

3.2. Adipogenesis-dependent nuclear localization of EWS

We next characterized the subcellular distribution of EWS during adipogenesis. Differentiation was induced in 3T3-L1

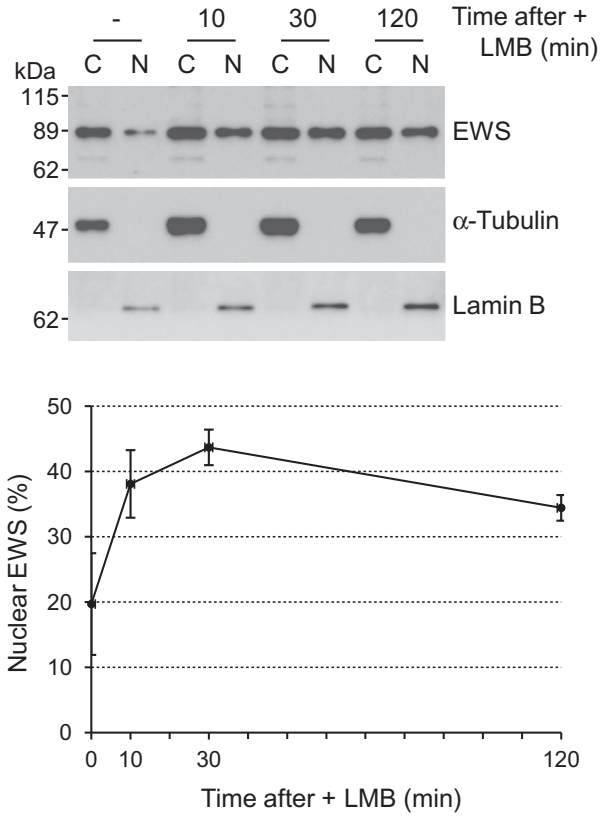

Fig. 1. The majority of EWS is regulated to localize stably in the cytosol in 3T3-L1 preadipocytes. The cells were treated with leptomycin B (LMB, 20 ng/mL) for the indicated time. (Upper panel) The subcellular fractions were immunoblotted for EWS. α-Tubulin and lamin B were used as cytosolic (C) and nuclear (N) markers, respectively. Representative blots are shown. (Lower panel) relative nuclear EWS levels obtained by densitometric analysis of the blots are shown. Data are the mean ± standard deviation (n = 3).

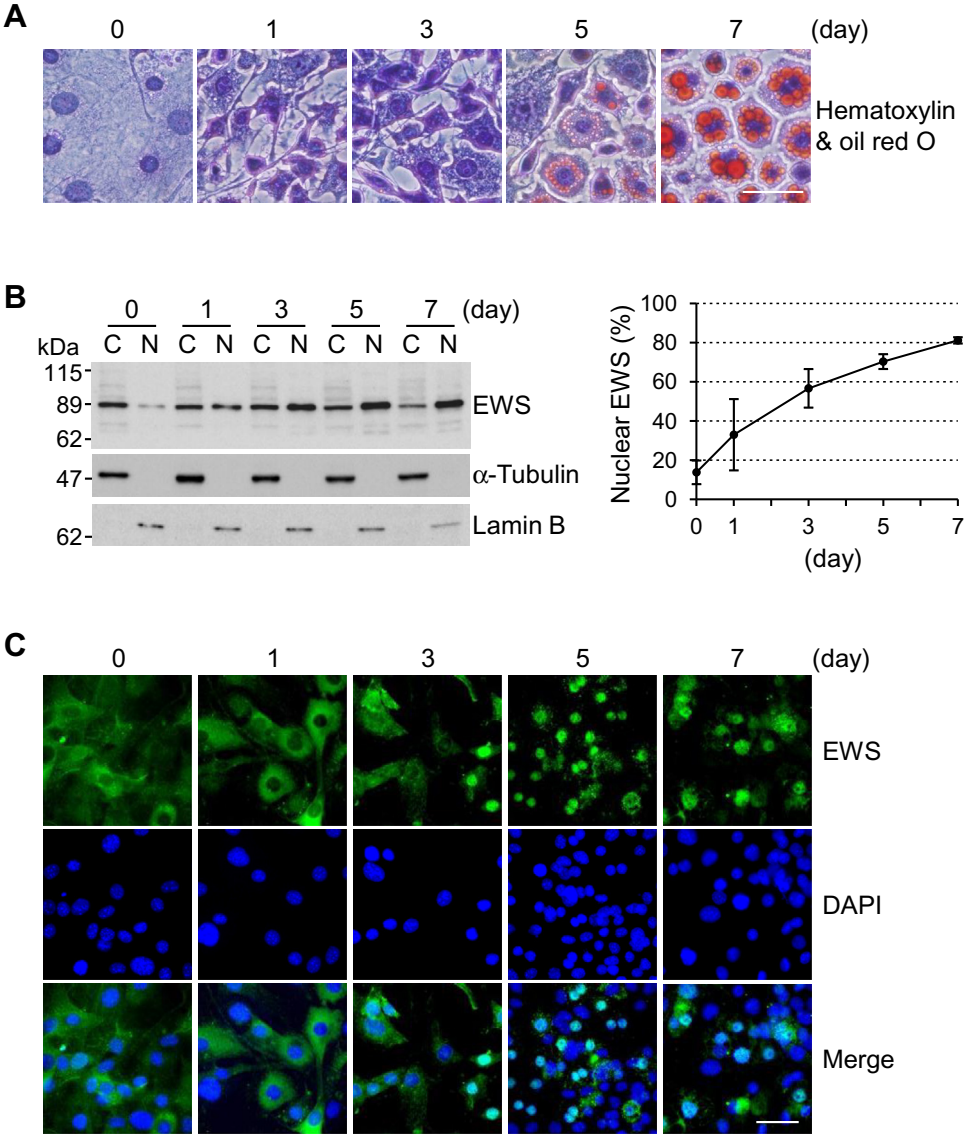

Fig. 2. Adipogenesis-dependent nuclear localization of EWS. Differentiation was induced in 3T3-L1 preadipocytes for 7 days. (A) The cells were stained with oil red O and hematoxylin. Bar, 100 μm. (B) Left panel shows representative western blots of the subcellular fractions probed with the indicated antibodies (C, cytosolic fraction; N, nuclear fraction). Right panel shows the relative nuclear EWS levels obtained by densitometric analysis of the blots. Data are the mean ± standard deviation ($n = 3$). (C) Representative image of differentiating cells immunostained with an anti-EWS (SAB2500370) antibody (green) and counterstained with DAPI (blue). Bar, 40 μm. (For interpretation of the references to color in this figure legend, the reader is referred to the web version of this article.)

preadipocytes until day 7, and the subcellular distribution of EWS was monitored. An adipogenesis-dependent increase in lipid droplet size was observed (Fig. 2A). Upon the induction of adipogenic differentiation, C/EBPβ, which is a critical transcription factor for adipogenesis, was expressed on and after day 1, while another adipogenic transcription factor, C/EBPα, was expressed on and after day 5 (data not shown), as we reported previously [16]. Biochemical subcellular fractionation showed that the nuclear localization of EWS was promoted upon differentiation, and the distribution of EWS in the nuclear fraction takes precedence over its cytosolic localization as adipogenesis advances (Fig. 2B). Consistent with the subcellular fractionation analysis, the majority of EWS in preadipocytes showed a diffuse cytoplasmic distribution by immunostaining and its distribution shifted from the cytoplasm to the nucleus with the progression of adipogenesis (Fig. 2C). These results indicate that adipogenic stimuli induce the nuclear localization of EWS.

3.3. Adipogenesis-dependent increase in the O-GlcNAc glycosylation, but not tyrosine phosphorylation, of EWS correlates with its nuclear distribution

Since 3T3-L1 cells maintain a steady level of EWS expression during adipogenesis as we reported previously [16] and EWS is a relatively stable protein with a half-life of approximately 19.6 h (Fig. S1), the adipogenesis-dependent nuclear localization of EWS might be regulated by post-translational modifications. It has been proposed that tyrosine phosphorylation of the C-terminal PY-NLS is a critical factor for the transportin-mediated nuclear import of EWS [17]. We examined tyrosine phosphorylation of EWS during adipogenesis, but this modification was undetectable throughout this process (Fig. 3A). Tyrosine phosphorylation of endogenous EWS was barely detectable in human embryonic kidney 293T cells but that was undetectable in 3T3-L1 preadipocytes even in the presence of sodium orthovanadate, a broad-spectrum tyrosine phosphatase

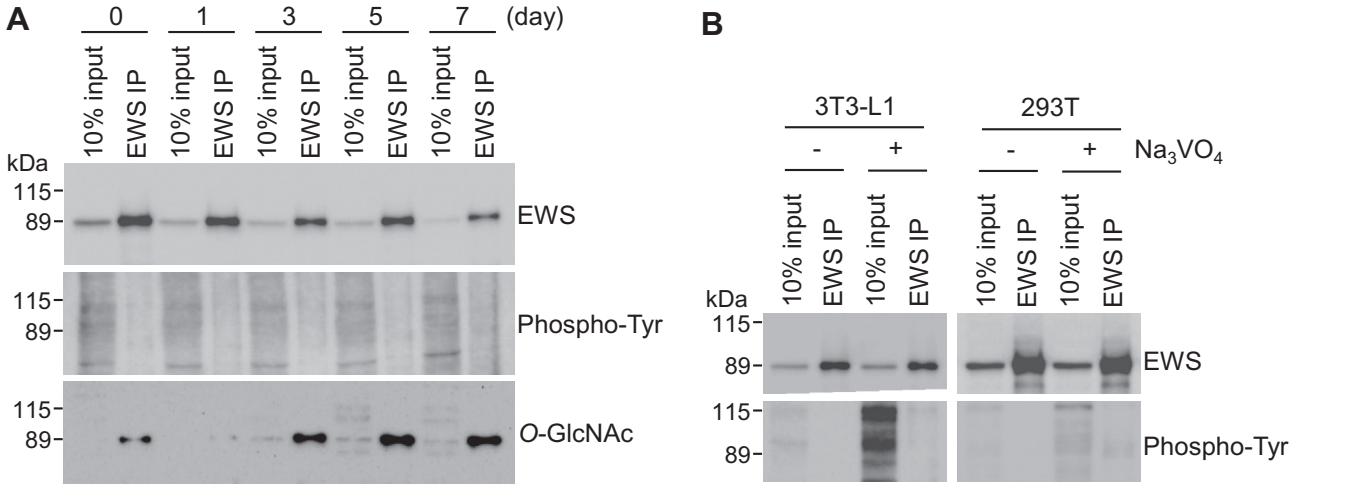

Fig. 3. Adipogenesis-dependent increase of the *O*-GlcNAcylation, but not tyrosine phosphorylation, of EWS. (A) Differentiation was induced 3T3-L1 preadipocytes for 7 days. EWS was immunoprecipitated (IP) from harvested whole cell lysates with an anti-EWS (G-5) antibody and the immunoprecipitates were immunoblotted with the indicated antibodies. (B) 3T3-L1 preadipocytes and human embryonic kidney 293T cells were cultured in the absence or presence of 2 mM sodium orthovanadate (Na_3VO_4) for 2 h. EWS was immunoprecipitated from harvested whole cell lysates with G-5 and the immunoprecipitates were immunoblotted with the indicated antibodies.

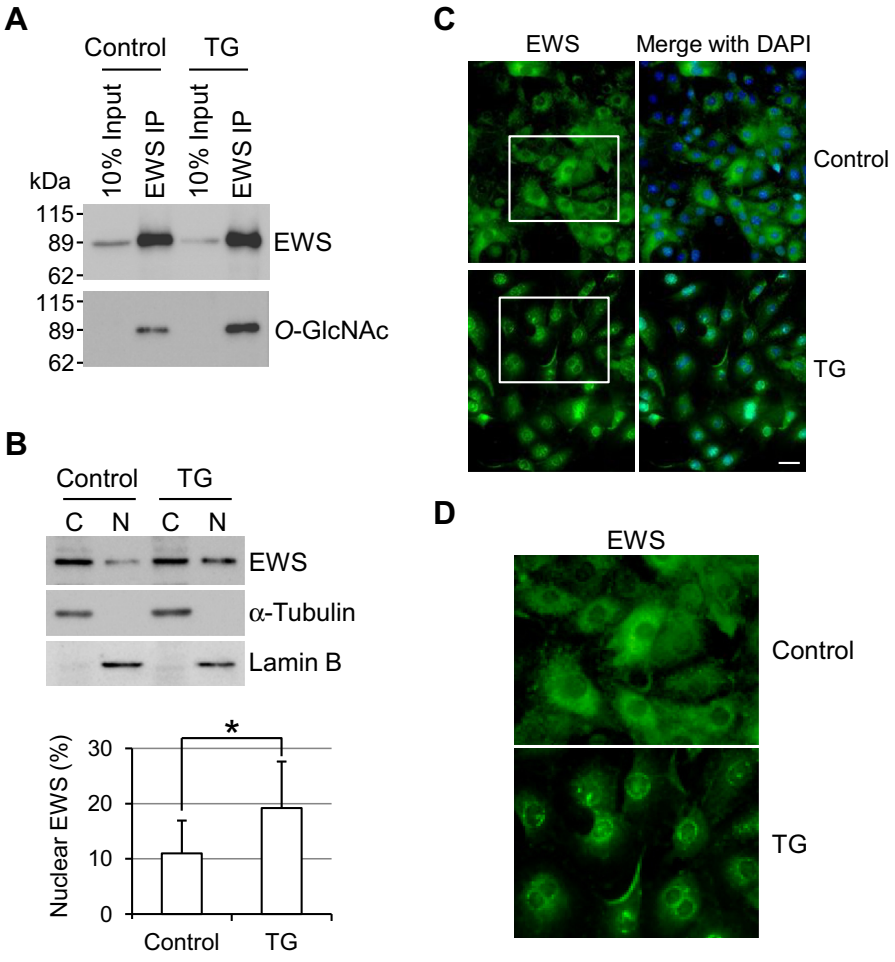

Fig. 4. *O*-GlcNAc glycosylation promotes the perinuclear localization of EWS. 3T3-L1 preadipocytes were cultured in the absence or presence of 100 nM thiamet G (TG) for 6 h. (A) EWS was immunoprecipitated (IP) from harvested whole cell lysates with an anti-EWS (G-5) antibody and the immunoprecipitates were immunoblotted with the indicated antibodies. (B) Upper panel shows representative western blots of the subcellular fractions probed with the indicated antibodies. C, cytosolic fraction; N, nuclear fraction. Lower panel shows relative nuclear EWS levels obtained by densitometric analysis of the blots. Data are the mean ± standard deviation ($n = 3$). $^{*}p < 0.036$. (C) Representative image of the cells immunostained with an anti-EWS (SAB2500370) antibody (green) and counterstained with DAPI (blue). Bar, 40 μm. (D) Enlarged views of the boxed regions in (C). (For interpretation of the references to color in this figure legend, the reader is referred to the web version of this article.)

inhibitor (Fig. 3B). Therefore, we concluded that tyrosine phosphorylation of PY-NLS appears not to have a critical role in the adipogenesis-dependent nuclear import of EWS in 3T3-L1 cells.

Previously, we used the wheat germ agglutinin-affinity pull-down assay to show that the levels of *O*-GlcNAc glycosylation of EWS in 3T3-L1 adipocytes are higher than in preadipocytes [16]. In the present study, we confirmed this finding by western blotting with an anti-*O*-GlcNAc antibody (Fig. 3A). This observation indicates that there is a correlation between the adipogenesis-dependent increase in EWS glycosylation and the increase in its nuclear distribution, and that *O*-GlcNAc glycosylation may play a regulatory role in the nuclear localization of EWS.

3.4. O-GlcNAc glycosylation stimulates the perinuclear localization of EWS

To examine whether the increase in the *O*-GlcNAc glycosylation of EWS affects its subcellular distribution, 3T3-L1 preadipocytes were treated with thiamet G, a potent and specific *O*-GlcNAcase inhibitor [18]. Six hours of thiamet G treatment resulted in an approximately 2-fold increase in the glycosylation of EWS (Fig. 4A). Biochemical subcellular fractionation showed that thiamet G treatment promoted a statistically significant increase in the nuclear distribution of EWS by approximately 2-fold (Fig. 4B). A similar result was obtained with another *O*-GlcNAcase inhibitor, PUGNAc (data not shown). Interestingly, microscopic observation revealed that thiamet G treatment induces the perinuclear localization of EWS (Fig. 4C and D). This result indicates that the *O*-GlcNAc glycosylation stimulates the recruitment of EWS to the periphery of the nuclear pore rather than its nuclear import. *In silico O*-GlcNAc glycosylation site analysis using the YinOYang 1.2 server (http://www.cbs.dtu.dk/services/YinOYang/) [19] predicted that 54 Ser/Thr residues of mouse EWS are possible modification sites and these putative sites are unevenly distributed in the N-terminus (Fig. S2). Although we do not have any data indicating the actual glycosylation sites of EWS in 3T3-L1 cells at the present time, EWS will be glycosylated at multiple sites in its N-terminus upon the induction of adipogenic differentiation. EWS is composed of a transactivation domain at the N-terminus and RNA recognition motifs at its C-terminus. Although the regulatory mechanism for the subcellular localization of EWS is less clear, the N-terminal R7BS domain and 3 independent C-terminal domains, including the third RGG motif, the zinc-finger motif, and the PY-NLS, are important for its efficient nuclear localization [2,11,14]. Since 12 out of the 54 possible glycosylation sites are located in the N-terminal R7BS domain, the nuclear localization potency of this domain might be regulated by glycosylation. Further study is needed to prove this hypothesis.

Recently, it was shown that EWS mediates the maturation of *let-7g* [7], which is an important microRNA for 3T3-L1 adipogenesis [20]. The adipogenesis-dependent nuclear localization of EWS that we found in this study may help to elucidate the molecular mechanism of microRNA processing mediated by EWS during adipogenesis. Furthermore, the cell cycle-dependent dynamic subcellular distribution of EWS in Cos7, HeLa, and human embryonic kidney 293T cells has been reported [13]. EWS has also been identified in cytoplasmic inclusions in the brain of a subset of patients with frontotemporal lobar degeneration [21,22]. Therefore, the regulatory mechanism for the localization of EWS in other cell lineages, including neuronal cells, is an important matter that should be explored.

Acknowledgment

We are grateful to Dr. Gerald W. Hart (Johns Hopkins University School of Medicine) for the kind gift of the anti-*O*-GlcNAc (CTD110.6) antibody.

Appendix A. Supplementary data

Supplementary data associated with this article can be found, in the online version, at http://dx.doi.org/10.1016/j.bbrc.2014.06.013.

References

[1] A. Bertolotti, T. Melot, J. Acker, M. Vigneron, O. Delattre, L. Tora, EWS, but not EWS-FLI-1, is associated with both TFIID and RNA polymerase II: interactions between two members of the TET family, EWS and hTAFII68, and subunits of TFIID and RNA polymerase II complexes, Mol. Cell Biol. 18 (1998) 1489–1497.
[2] K.L. Rossow, R. Janknecht, The Ewing's sarcoma gene product functions as a transcriptional activator, Cancer Res. 61 (2001) 2690–2695.
[3] N. Araya, K. Hirota, Y. Shimamoto, M. Miyagishi, E. Yoshida, J. Ishida, S. Kaneko, M. Kaneko, T. Nakajima, A. Fukamizu, Cooperative interaction of EWS with CREB-binding protein selectively activates hepatocyte nuclear factor 4-mediated transcription, J. Biol. Chem. 278 (2003) 5427–5432.
[4] L. Yang, H.A. Chansky, D.D. Hickstein, EWS-Fli-1 fusion protein interacts with hyperphosphorylated RNA polymerase II and interferes with serine–arginine protein-mediated RNA splicing, J. Biol. Chem. 275 (2000) 37612–37618.
[5] M. Dutertre, G. Sanchez, M.-C. de Cian, J. Barbier, E. Dardenne, L. Gratadou, G. Dujardin, C. le Jossic-Corcos, L. Corcos, D. Auboeuf, Cotranscriptional exon skipping in the genotoxic stress response, Nat. Struct. Mol. Biol. 17 (2010) 1358–1366.
[6] M.P. Paronetto, B. Miñana, J. Valcárcel, The Ewing sarcoma protein regulates DNA damage-induced alternative splicing, Mol. Cell 43 (2011) 353–368.
[7] E.J. Sohn, J. Park, S.-I. Kang, Y.-P. Wu, Accumulation of pre-let-7g and downregulation of mature let-7g with the depletion of EWS, Biochem. Biophys. Res. Commun. 426 (2012) 89–93.
[8] L. Huang, I. Kuwahara, K. Matsumoto, EWS represses cofilin 1 expression by inducing nuclear retention of cofilin 1 mRNA, Oncogene (2013), http://dx.doi.org/10.1038/onc.2013.255.
[9] K.Y. Kim, Y.J. Hwang, M.-K. Jung, J. Choe, Y. Kim, S. Kim, C.-J. Lee, H. Ahn, J. Lee, N.W. Kowall, Y.K. Kim, J.-I. Kim, S.B. Lee, H. Ryu, A multifunctional protein EWS regulates the expression of Drosha and microRNAs, Cell Death Differ. 21 (2014) 136–145.
[10] J.S. Felsch, W.S. Lane, E.G. Peralta, Tyrosine kinase Pyk2 mediates G-protein-coupled receptor regulation of the Ewing sarcoma RNA-binding protein EWS, Curr. Biol. 9 (1999) 485–488.
[11] R.P. Zakaryan, H. Gehring, Identification and characterization of the nuclear localization/retention signal in the EWS proto-oncoprotein, J. Mol. Biol. 363 (2006) 27–38.
[12] M.K. Andersson, A. Ståhlberg, Y. Arvidsson, A. Olofsson, H. Semb, G. Stenman, O. Nilsson, P. Åman, The multifunctional FUS, EWS and TAF15 proto-oncoproteins show cell type-specific expression patterns and involvement in cell spreading and stress response, BMC Cell Biol. 9 (2008) 37.
[13] R.P. Leemann-Zakaryan, S. Pahlich, M.J. Sedda, L. Quero, D. Grossenbacher, H. Gehring, Dynamic subcellular localization of the Ewing sarcoma proto-oncoprotein and its association with and stabilization of microtubules, J. Mol. Biol. 386 (2009) 1–13.
[14] D.J. Shaw, R. Morse, A.G. Todd, P. Eggleton, C.L. Lorson, P.J. Young, Identification of a tripartite import signal in the Ewing sarcoma protein (EWS), Biochem. Biophys. Res. Commun. 390 (2009) 1197–1201.
[15] L.L. Belyanskaya, P.M. Gehrig, H. Gehring, Exposure on cell surface and extensive arginine methylation of Ewing sarcoma (EWS) protein, J. Biol. Chem. 276 (2001) 18681–18687.
[16] K. Ishihara, I. Takahashi, Y. Tsuchiya, M. Hasegawa, K. Kamemura, Characteristic increase in nucleocytoplasmic protein glycosylation by *O*-GlcNAc in 3T3-L1 adipocyte differentiation, Biochem. Biophys. Res. Commun. 398 (2010) 489–494.
[17] R.P. Leemann-Zakaryan, S. Pahlich, D. Grossenbacher, H. Gehring, Tyrosine phosphorylation in the C-terminal nuclear localization and retention signal (C-NLS) of the EWS protein, Sarcoma (2011), http://dx.doi.org/10.1155/2011/218483.
[18] S.A. Yuzwa, M.S. Macauley, J.E. Heinonen, X. Shan, R.J. Dennis, Y. He, G.E. Whitworth, K.A. Stubbs, E.J. McEachern, G.J. Davies, D.J. Vocadlo, A potent mechanism-inspired *O*-GlcNAcase inhibitor that blocks phosphorylation of tau *in vivo*, Nat. Chem. Biol. 4 (2008) 483–490.
[19] R. Gupta, S. Brunak, Prediction of glycosylation across the human proteome and the correlation to protein function, Pac. Symp. Biocomput. 7 (2002) 310–322.
[20] T. Sun, M. Fu, A.L. Bookout, S.A. Kliewer, D.J. Mangelsdorf, MicroRNA *let-7* regulates 3T3-L1 adipogenesis, Mol. Endocrinol. 23 (2009) 925–931.
[21] M. Neumann, E. Bentmann, D. Dormann, A. Jawaid, M. Dejesus-Hernandez, O. Ansorge, S. Roeder, H.A. Kretzschmar, D.G. Munoz, H. Kusaka, O. Yokota, L.-C. Ang, J. Bilbao, R. Rademakers, C. Haass, I.R.A. Mackenzie, FET proteins TAF15 and EWS are selective markers that distinguish FTLD with FUS pathology from amyotrophic lateral sclerosis with *FUS* mutations, Brain 134 (2011) 2595–2609.
[22] Y.S. Davidson, A.C. Robinson, Q. Hu, M. Mishra, A. Baborie, E. Jaros, R.H. Perry, N.J. Cairns, A. Richardson, A. Gerhard, D. Neary, J.S. Snowden, E.H. Bigio, D.M.A. Mann, Nuclear carrier and RNA binding proteins in frontotemporal lobar degeneration associated with fused in sarcoma (FUS) pathological changes, Neuropathol. Appl. Neurobiol. (2012), http://dx.doi.org/10.1111/j.1365-2990.2012.01274.x.